Journal of Computational and Applied Mechanics, Vol. 15, No. 1, (2020), pp. 15–26
DOI: 10.32973/jcam.2020.002

AN INVESTIGATION ON TRANSMISSION LOSS OF CLAMPED DOUBLED THIN PLATE WITH ADDED MASS

Akintoye Olumide Oyelade
Department of Civil and Environmental Engineering,
University of Lagos, Akoka, Lagos, Nigeria
aoyelade@unilag.edu.ng

[Received: March 16, 2019, Accepted: May 12, 2020]

Abstract. Thin plate acoustic metamaterials (TAM) have demonstrated uncommon capacity in controlling low-frequency sound transmission. This paper concentrates on a theoretical and experimental investigation of clamped double polylactic acid (PLA) thin plates with attached mass. The theoretical formulation was done using a rectangular duct below the first cut off frequency. The sound transmission loss (STL) of the plates is calculated for plane wave condition, then the accuracy and capability of the theoretical model is verified through the comparison with the finite element method and experiment. The influence of several key parameters on the STL of the double-panel configuration is then systematically studied, including thickness of air cavity, magnitude of mass attached, and mode shapes. New peak and dip frequencies are found for the TAM with attached masses. The developed model can serve as an efficient tool for the design of such thin plate metamaterials.

Mathematical Subject Classification: 74H45, 74K20
Keywords: Polylactic acid, acoustic metamaterials, sound transmission loss, clamped plate

1. Introduction

Double-leaf partition membranes and thin plates structures have found increasingly wide applications in sound control engineering due to their superior sound insulation capability over single-leaf configurations. Typical examples include automotive, marine, aircraft, construction industries and so on [1–3]. Double-wall structures, however, are less efficient at low frequency around the mass–air–mass resonance at which the model for infinite panels reveals an out-of-phase motion of the two walls [4]. Until quite recently, there has been a persistent effort to explore the prospect of using acoustic metamaterials to increase the transmission loss of double-wall partitions at low frequencies [5, 6]. In these works, analytical and numerical investigation of the STL features are controlled by the magnitude of the added mass and/or pretension of the membrane. However, only the effect of mass and tensions were examined, and no further detailed analysis and experimental verification were presented. Thus, to the author's best knowledge, very few experimental studies have been reported on the coupled vibroacoustic problems of double thin plates with added mass in a rigid duct, and that would be solved in this paper. The thin plate acoustic metamaterial (TAM) can be described as an elastic plate carrying a concentrated mass or masses on each side. The vibration eigenfrequencies of the thin plate acoustic metamaterials

(TAM) can be tuned by varying the thin plate and mass properties. In this paper, we present the experimental realization and theoretical understanding of a double thin plate metamaterial with one mass resonator on each face to further study and verify the work carried out previously numerically. What distinguishes this study from others is that the effect of cavity gaps in relation with the attached mass and the mode shapes characteristics of the plates are investigated. In the first instance, a brief overview of the structural and acoustic models is presented. Results for the experiments, theory and numerical investigation are then presented and discussed, followed by concluding remarks.

2. Theoretical formulation

Consider now TAM, as shown in Figure 1(a), where the thin plate is attached by N point masses on each plate. The case of $N = 1$ is illustrated in Figure 1(b), and the mass is located at (x_h, y_h). The upper plate is excited by a plane harmonic sound wave. The two elastic thin plates are fully clamped along their edges to an infinite rigid acoustic baffle.

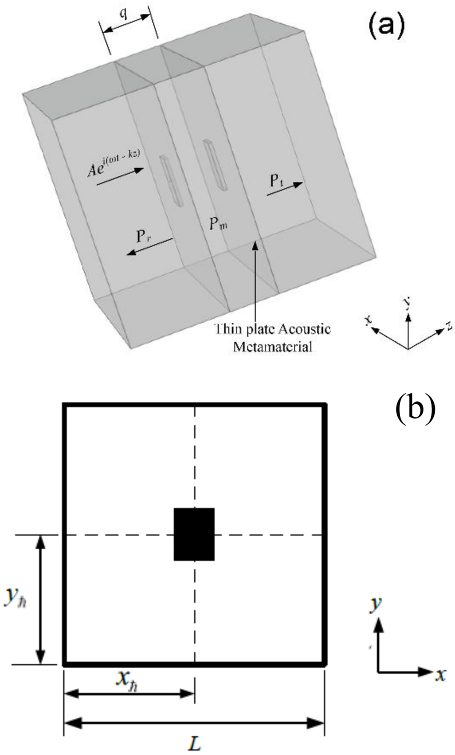

Figure 1. (a) TAM subjected to a plain wave loading in a rectangular duct (b) TAM attached with a centrally placed mass

The flexural motions equation of two thin plates connected each by N number of point masses and air cavity is given by

$$D_1\nabla^4\bar{\xi}_1 - M_1\omega^2\bar{\xi}_1 - \sum_{\hbar=1}^{N}\overset{\leftarrow}{\bar{M}}_1\omega^2\bar{\xi}_1\delta\left\{x-x_\hbar, y-y_\hbar\right\} =$$

$$= 2A + \sum_{m=0}^{N_m}\sum_{n=0}^{N_n}\left[e_{mn}-b_{mn}-c_{mn}\right]\cos\left(\pi m x/L\right)\cos\left(\pi n x/L\right) \quad (1)$$

for panel 1, and

$$D_2\nabla^4\bar{\xi}_2 - \overset{\leftarrow}{M}_2\omega^2\bar{\xi}_2 - \sum_{\hbar=1}^{N}\overset{\leftarrow}{\bar{M}}_2\omega^2\bar{\xi}_2\delta\left\{x-x_\hbar, y-y_\hbar\right\} =$$

$$= \sum_{m=0}^{N_m}\sum_{n=0}^{N_n}\left[b_{mn}e^{-ik_zq}+c_{mn}e^{ik_zq}-d_{mn}e^{-ik_zq}\right]\cos\left(\pi m x/L\right)\cos\left(\pi n x/L\right) \quad (2)$$

for panel 2. In the above equations $\bar{\xi}_1$, D_1, M_1 and $\bar{M}_1$ are the transverse displacement, the flexible rigidity, the mass density and the discrete mass (attached) of panel 1, respectively. Symbols with subscript 2 have the same meanings as defined above but applied to panel 2. e_{mn}, b_{mn}, c_{mn}, d_{mn} and A are amplitude constants related to the waves in the duct as shown in Figure 1. This is given by Kim et al. [7]:

$$Q_1 = Ae^{i(\omega t+k_z z)} + \sum_{m=0}^{N_r}\sum_{n=0}^{N_s} e_{mn}e^{i(\omega t+k_z z)}\cos\left(\pi m x/L\right)\cos\left(\pi n x/L\right)\ , \quad (3)$$

$$Q_2 = \sum_{m=0}^{N_r}\sum_{n=0}^{N_s}\left[b_{mn}e^{i(\omega t-k_z z)}+c_{mn}e^{i(\omega t+k_z z)}\right]\cos\left(\pi m x/L\right)\cos\left(\pi n x/L\right)\ , \quad (4)$$

$$Q_3 = \sum_{m=0}^{N_r}\sum_{n=0}^{N_s} d_{mn}e^{i(\omega t-k_z z)}\cos\left(\pi m x/L\right)\cos\left(\pi n x/L\right)\ , \quad (5)$$

where L is the height of the plate, ω is the angular frequency, and $i=\sqrt{-1}$. Wave number k_z in z direction satisfies the following relation:

$$k_z = \left[k^2 - \frac{\pi^2\left(m^2+n^2\right)}{L^2}\right]^{1/2}, \quad (6)$$

which shows that the axial wavenumber k_z depends on m and n. When m = n = 0, which can be recognized as the one-dimensional sound field assumed in this work. The plane wave is the fundamental duct mode. The displacement of the plates can be expressed as a harmonic function:

$$\xi_1{=}\bar{\xi}_1 e^{i\omega t}, \xi_2{=}\bar{\xi}_2 e^{i\omega t} \,. \tag{7}$$

At the air panel interface, the boundary conditions at thin plate surfaces give

$$\frac{1}{\rho}\frac{\partial Q}{\partial z} = -\frac{\partial^2 \xi_1}{\partial t^2} = \omega^2 \xi_1 \qquad \text{at} \qquad z = 0 \,, \tag{8}$$

$$\frac{1}{\rho}\frac{\partial Q}{\partial z} = -\frac{\partial^2 \xi_2}{\partial t^2} = \omega^2 \xi_2 \qquad \text{at} \qquad z = q \,, \tag{9}$$

where ρ is the density of air. For clamped plates, the flexural displacements of the incident and radiating plates can be expressed as

$$\bar{\xi}_1 \left(x, y\right) = \sum_{j=1}^{7} a_j \Phi_j \left(x, y\right), \bar{\xi}_2 \left(x, y\right) = \sum_{j=1}^{7} T_j \Phi_j \left(x, y\right), \tag{10}$$

where $\Phi_j \left(x, y\right)$ is the j^{th} mode of the clamped plate. Approximate solution for the first 36-term modes as proposed by Young [8] is defined as

$$\Phi_j \left(x, y\right) = \sum_{r=1}^{6} \sum_{s=1}^{6} A_{rs}^{j} \phi_r \left(x\right) \phi_s \left(y\right), \tag{11}$$

where $\phi_r \left(y\right)$ is the r^{th} mode of the clamped beam vibration defined by the following relation:

$$\phi_r \left(x\right) = \cosh\left(\varepsilon_r x/L\right) - \cos\left(\varepsilon_r x/L\right) - \alpha_r \left\{sinh\left(\varepsilon_r x/L\right) - \sin\left(\varepsilon_r x/L\right)\right\} \tag{12}$$

in which parameter ε_r and α_r can be found in mechanics books [9, 10]. The natural frequency corresponding to the j^{th} mode is given by

$$\omega_j = \frac{\lambda_j h}{L^2} \sqrt{\frac{E}{12\rho_p \left(1 - v^2\right)}}, \tag{13}$$

where h, E, ν and ρ_p are the thickness, Young modulus, Poisson ratio and density of the plate. The coefficients A_{rs}^{j} and λ_j are found in Leissa [11]. Using displacement functions in equation (7), equations (1) and (2) become

$$\sum_{j=1}^{7} \overleftarrow{M}_1 a_j \left\{\omega_j^2 - \omega^2\right\} \Phi_j - \sum_{\hbar=1}^{N} \overleftarrow{M}_1 \omega^2 a_j \delta \left\{x - x_\hbar, y - y_\hbar\right\} \Phi_j =$$

$$= 2A - 2 \sum_{m=0}^{N_m} \sum_{n=0}^{N_n} b_{mn} \cos\left(\pi m x/L\right) \cos\left(\pi n x/L\right) \,, \tag{14}$$

$$\sum_{j=1}^{7} \overleftarrow{M}_2 T_j \left\{\Omega_j^2 - \omega^2\right\} \Phi_j - \sum_{\hbar=1}^{N} \overleftarrow{M}_2 \omega^2 T_j \delta \left\{x - x_\hbar, y - y_\hbar\right\} \Phi_j$$
$$= 2 \sum_{m=0}^{N_m} \sum_{n=0}^{N_n} c_{mn} e^{ik_z q} \cos\left(\pi m x / L\right) \cos\left(\pi n x / L\right) , \quad (15)$$

where ω_j and Ω_j are the natural frequencies of the j^{th} mode of plates 1 and 2, respectively. Multiply this equation by $\Phi_M(x, y)$ and integrate over the entire region. Then combining the acoustic part at low frequency can be obtained as [12]:

$$\overleftarrow{M}_1 \Gamma_{jM} \left(\omega_j^2 - \omega^2\right) a_j - \overleftarrow{M}_1 \omega^2 a_j Z_{jM} = 2\beta_{M,00} \left(A - b_{00}\right) , \quad (16)$$

$$\overleftarrow{M}_2 \Gamma_{jM} \left(\Omega_j^2 - \omega^2\right) T_j - \overleftarrow{M}_2 \omega^2 T_j Z_{jM} = 2c_{00} \beta_{M,00} e^{ikq} , \quad (17)$$

$$b_{00} - c_{00} = \sum_{j=1}^{7} i\rho c \omega a_j \beta_{j,00} , \quad (18)$$

$$b_{00} e^{-ikq} - c_{00} e^{ikq} = \sum_{j=1}^{7} i\rho c \omega T_j \beta_{j,00} , \quad (19)$$

where

$$\begin{aligned}
\Gamma_{jM} &= \frac{1}{L^2} \int_A \Phi_j\left(x, y\right) \Phi_M\left(x, y\right) \mathrm{d}x \, \mathrm{d}y , \\
Z_{jM} &= \frac{1}{L^2} \sum_{ka=1}^{N} \left(\Phi_j\left(x_\hbar, y_\hbar\right) \Phi_M\left(x_\hbar, y_\hbar\right)\right) , \\
\beta_{M,rs} &= \frac{1}{L^2} \int_A \cos\left(\frac{\pi r x}{L}\right) \cos\left(\frac{\pi s y}{L}\right) \Phi_M\left(x, y\right) \mathrm{d}x \, \mathrm{d}y .
\end{aligned} \quad (20)$$

Equations (16), (17), (18) and (19) can be combined in matrix form:

$$\begin{bmatrix} L_{11} & 0 & L_{13} & 0 \\ 0 & L_{22} & 0 & L_{24} \\ L_{31} & L_{32} & L_{33} & L_{34} \\ 0 & L_{42} & L_{43} & L_{44} \end{bmatrix} \begin{Bmatrix} A \\ B \\ C \\ D \end{Bmatrix} = \begin{Bmatrix} F \\ 0 \\ 0 \\ 0 \end{Bmatrix} \quad (21)$$

where the coefficients $L_{11}, \ldots, L_{44}$ ar given by the following equations:

$$\begin{aligned}
&L_{11} = \overleftarrow{M}_1 \left(\omega_j^2 - \omega^2\right) \Gamma_{jM} - \hat{m}_1 \omega^2 Z_{jM} \,, && L_{13} = 2\beta_{M,00} \,, \\
&L_{22} = \overleftarrow{M}_2 \left(\Omega_j^2 - \omega^2\right) \Gamma_{jM} - \hat{m}_2 \omega^2 Z_{jM} \,, && L_{24} = -2\beta_{M,00} e^{ikq} \,, \\
&L_{31} = -i\rho c \omega \beta_{j,00} \,, && L_{33} = -1 \,, \\
&L_{34} = -1 \,, && L_{42} = -i\rho c \omega \beta_{j,00} \,, \\
&L_{43} = e^{-ikq} \,, && L_{44} = -e^{ikq} \,.
\end{aligned} \tag{22}$$

The elements of the displacement coefficient vectors A, B, C, D and the generalized force vector F take the form:

$$\begin{aligned}
A_{j\times 1} &= \{a_1, \ldots\ldots a_7\}^T \,, \quad & B_{j\times 1} &= \{T_1, \ldots\ldots T_7\}^T \,, \\
C &= b_{00} \,, & D &= c_{00} \,,
\end{aligned} \tag{23}$$

$$F_{M\times 1} = 2\beta_{M,00} \,, \qquad A = \{F_1, \ldots\ldots F_7\}^T \,. \tag{24}$$

Equation (22) describes the vibroacoustic behavior of the coupled system, which can be used to calculate various coefficients for constructing the displacement of each mode of the panels and the amplitudes inside the cavity. The sound transmission coefficient (tao) is expressed as:

$$\tau = \left| \frac{d_{00}}{A} \right|^2 = \left| \frac{b_{00} - c_{00} e^{2ikq}}{A} \right|^2 . \tag{25}$$

The sound transmission loss for a single incident wave, therefore, is calculated in decibel scale via

$$STL = -10 \log_{10} \left(\frac{1}{\tau} \right) . \tag{26}$$

3. Experimental investigation

3.1. **Experimental set up.** The experimental set up is shown in Figure 2. The procedure and the method of converting the rectangular plate to circular plate was established in our earlier paper [13]. Briefly explained, the apparatus consists of Bruel & Kjaer type 4206 impedance tubes with the sample sandwiched inbetween. The front tube has a loudspeaker at one end to generate a plane wave in the tube. There are two sensors in the front tube to sense the incident and reflected waves. The third sensor in the back tube, terminated with an anechoic sponge, senses the transmitted wave. The signals from the three sensors are sufficient to resolve the transmitted and reflected wave amplitudes [13]. The outer of the PLA plates is 120 mm while the inner diameter for the experiment is 100 mm. The experiment samples were attached to a sample holder in the tube to provide a reliable boundary condition for each experiment.

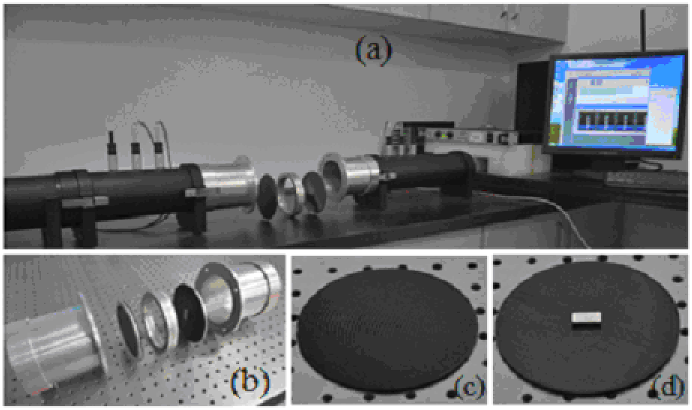

Figure 2. Experimental setup for STL measurements of fully clamped double-plates: (a) impedance tube (b) Sample holder, (c) Plain PLA, (d) Plain PLA with mass 2

3.2. **Validation.** Two test cases are considered in order to validate the theoretical model and numerical code developed in this study. Firstly, the present model is compared with results of Kim et al. [7] for plywood plate in Figure 3(a). The theoretical model for Kim et al. for rectangular plate was modeled using the parameters given, and the present model agree well for all frequencies. Secondly, STL predictions of the plain plate from the current model are compared with those obtained by using a commercially available FE code, COMSOL MultiphysicsTM and with experimental resuklts using circular PLA plates. The present model, the numerical solution, and experiment data agree as shown in Figure 3(b). There is little discrepancy at the second

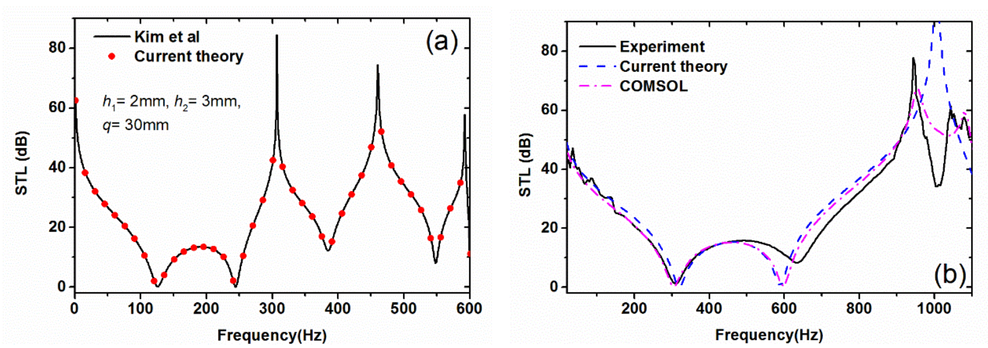

Figure 3. STL at low frequency of double PLA panel separated by air cavity without magnetic force: (a) comparison between the current study and Kim et al [7] (b) 1 mm thickness with 10 mm air cavity

resonance between the experiment and the current model. This discrepancy in the experimental values could be the result of the inability to accurately determine the air cavity gap in the experiment.

4. Results and discussion

The proposed analytical model is further applied for investigating the coupled vibroacoustic behaviour of the TAM. Consideration is paid to parameter effects such as thickness of plate, weight of the mass, cavity gap, and mode shapes of the plates on acoustic properties of the TAM. To quantify the effects of panel thickness, the STL versus frequency curve is presented in Figure 4. As expected, as the thickness increases the STL increases at low frequency. However, it is found that the frequency gap separation between the first and second resonances drops. This implies that as the thickness increases the acoustic resonance can be cancelled, even for the double plates. In addition, the current model as shown in Figure 4(b) is in close agreement with the

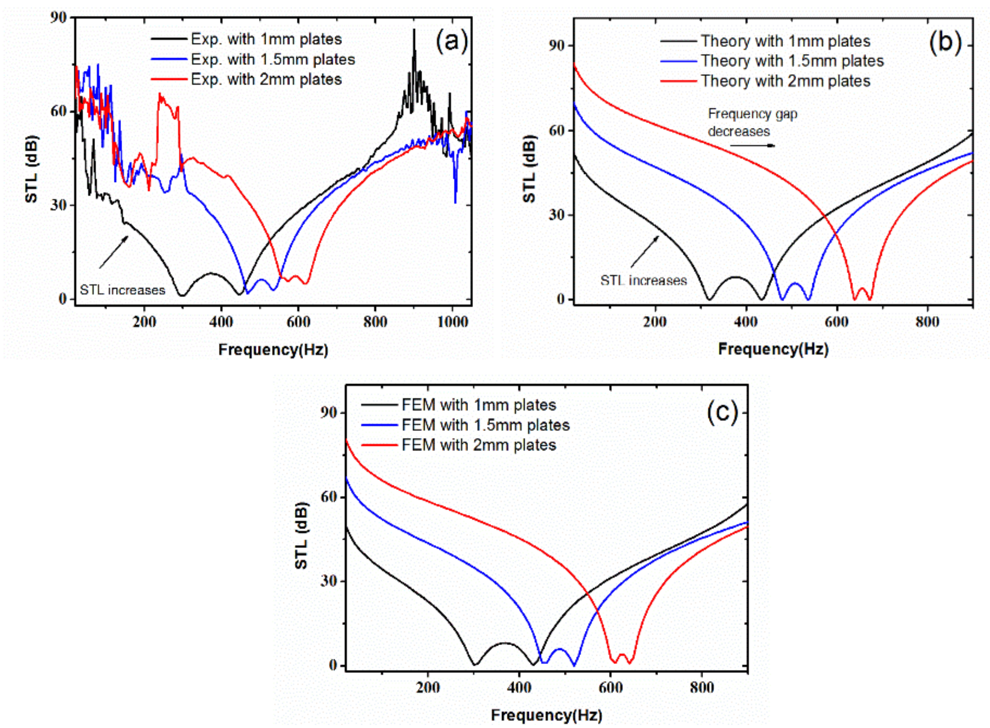

Figure 4. The effects of plate thickness on transmission loss 30 mm air cavity: (a) experimental data (b) theretical data and (c) FEM simulations

numerical mode. For example for a 1 mm thick PLA, the numerical simulation has 300 Hz and 430 Hz for the first and second resonance, respectively, while for the current model, it has 320 Hz and 435 Hz, respectively.

Figure 5 shows the comparison of STL spectra for the effect of different masses for the experiments, current model and FEM results. Firstly, the mass shifted the plate-cavity-plate resonance from 520–300 Hz for experiment results whereas the shift is from 480–210 Hz and 480–240 Hz for the theory and FEM, respectively. It is observed that with a heavier attached mass, STL summits and valleys move toward the low frequency regime. Secondly, there is multiple modes vibration after the second resonance in the experiment results which is not captured in the theoretical and FEM results. Hence, in this frequency range the value of STL for experiments is lower compared to theory and COMSOL results. The reason for the excitation of these modes could be attributed to an unevenly damped plate, and/or to the structural flanking path as discussed by Carneal and Fuller [2]. This contributed to the lower STL values obtained in the experiment.

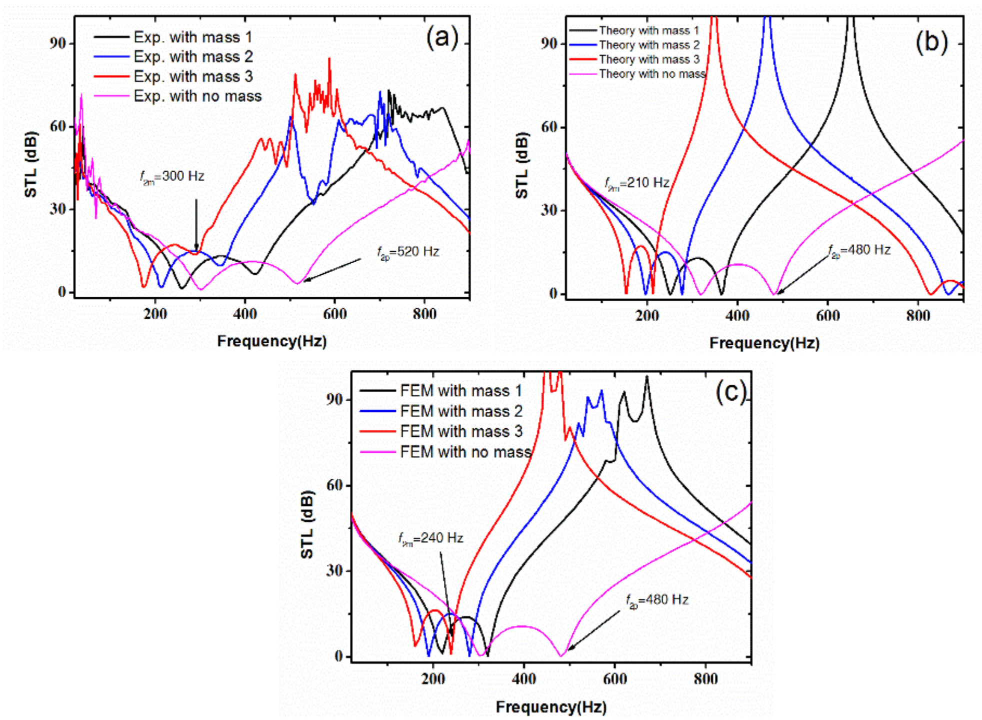

Figure 5. The effects of plate thickness on transmission loss of 30 mm air cavity as in Figure 4

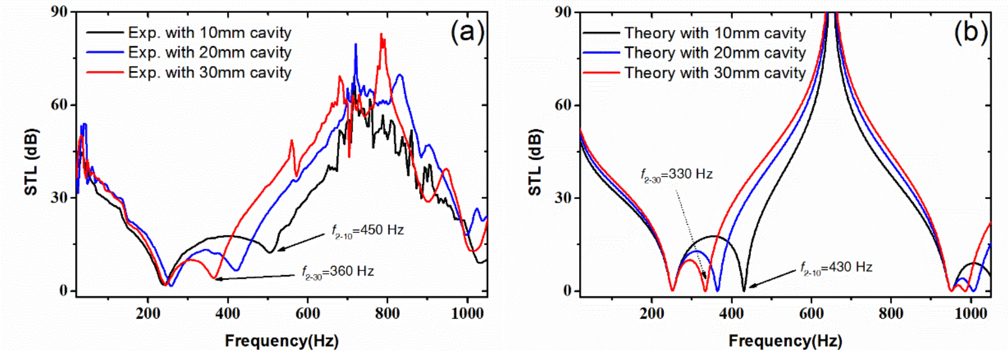

Figure 6. The effects of cavity gap on transmission loss: (a) transmission loss of 1 mm thick plate with mass 1 with different cavity gap (b) corresponding analytical solutions

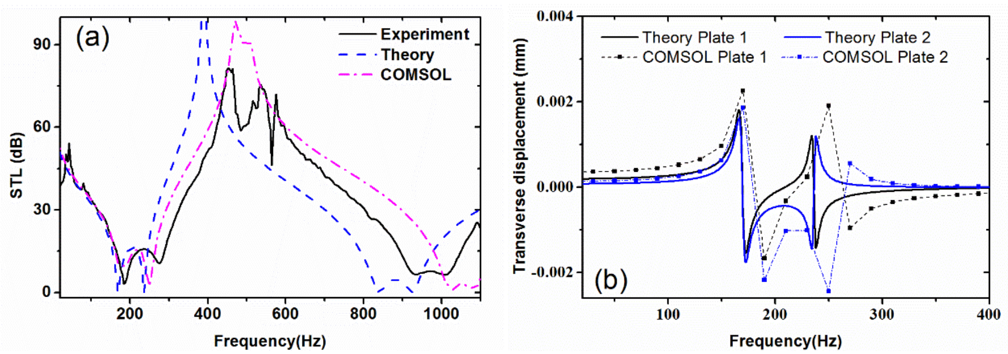

Figure 7. STL at low frequency of double PLA panel separated by air cavity with mass 2: (a) 1 mm thickness with 20 mm air cavity (b) transverse displacements for theory and FEM

The influence of the air cavity gap between the thin plates on the STL plot is displayed in Figure 6. The locations of mass-air-mass resonance shift to lower frequencies with increasing air cavity gap. The current model estimates the second resonance occurred around 430 and 330 Hz for 10 mm and 30 mm air cavity gap, respectively. The corresponding experiment occurred at 450 and 360 Hz respectively.

Figure 7 shows the STL spectra of double plates and their corresponding transverse displacement. The first two natural frequencies of the modes of TAMs obtained from the analytical method and FE analysis are $f_1^a = 170$ Hz, $f_2^a = 240$ Hz and $f_1^c = 179$ Hz and $f_2^a = 252.5$ Hz, respectively. The transverse displacement of the TAM shows that the incident panel and the radiating panel vibrate in out-of-phase between the structural and acoustic resonances. Very good agreement is observed for the first two resonant frequencies, which further confirms the accuracy and capability of the current analytical model. The corresponding mode shapes from the analytical method and FE analysis are also shown in Figure 8. Results show that the two methods generally yield similar results. However, the effect of using a lumped mass in the derivation of the analytical mode is obviously seen in Figure 8(a), where the surface displacement area is not as wide as we have in Figure 8(b).

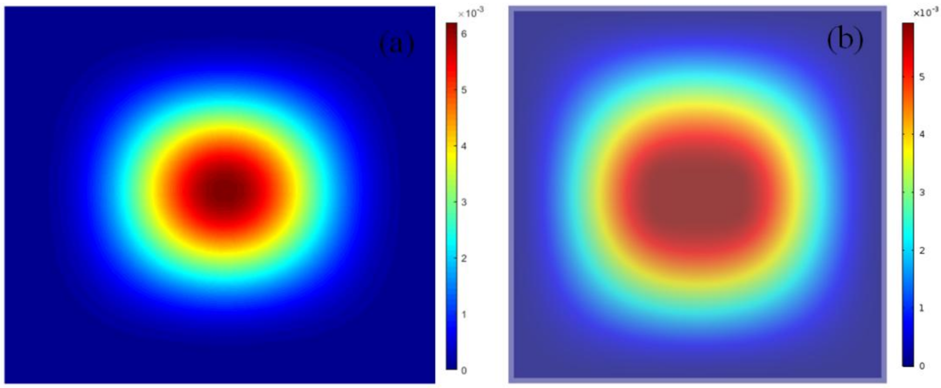

Figure 8. Panel deflection mode shapes of the TAM in Figure 6 under first resonance frequency: (a) analytical solution at $f_1^a = 170$ Hz, (b) COMSOL solution at $f_1^c = 179$ Hz

5. Conclusion

In this work, an analytical approach has been developed to investigate the vibroacoustic behavior of a finite double thin-plate attached with a mass in a rigid rectangular duct. Experimental measurements are subsequently performed to validate the theoretical predictions, with good overall agreement achieved for thin plates with mass and without mass. The influence of several key system parameters on the sound transmission loss capability of clamped double-thin plate panel has been systematically explored, including different mass magnitude, thickness of air cavity, and mode shapes.

References

1. J. P. Carneal and C. R. Fuller. "Active structural acoustic control of noise transmission through double panel systems." *AIAA Journal,* **33**, (1995), pp. 618–623. DOI: 10.2514/3.12623.
2. J. P. Carneal and C. R. Fuller. "An analytical and experimental investigation of active structural acoustic control of noise transmission through double panel systems." *Journal of Sound Vibration,* **272**, (2004), pp. 749–771. DOI: 10.1016/S0022-460X(03)00418-8.

3. Y. Liu and C. Daudin. “Analytical modelling of sound transmission through finite clamped double-wall sandwich panels lined with poroelastic materials.” *Composite Structures,* **172**, (2017), pp. 359–373. DOI: 10.1016/j.compstruct.2017.03.024.
4. L. Cheng, Y. Y. Li, and J. X. Gao. “Energy transmission in a mechanically-linked double-wall structure coupled to an acoustic enclosure.” *The Journal of the Acoustical Society of America,* **117**, (2005), pp. 2742–2751. DOI: 10.1121/1.1886525.
5. J. Chen, Y. Chen, H. Chen, and Y. Yeh. “Bandwidth broadening for transmission loss of acoustic waves using coupled membrane-ring structure.” *Materials Research Express,* **3**, (2016), pp. 1–10. DOI: 10.1088/2053-1591/3/10/105801.
6. Y. Chen, G. Huang, X. Zhou, G. Hu, and Sun C. T. “Analytical coupled vibroacoustic modeling of membrane-type acoustic metamaterials: Membrane model.” *The Journal of the Acoustical Society of America,* **136**, (2014), pp. 2926–2934. DOI: 10.1121/1.4892870.
7. H. S. Kim, S. R. Kim, S. H. Lee, Y. H. Seo, and P. S. Ma. “Sound transmission loss of double plates with an air cavity between them in a rigid duct.” *The Journal of the Acoustical Society of America,* **139**, (2016), 2324–2333. DOI: 10.1121/1.4946987.
8. D. Young. “Vibration of rectangular plates by the Ritz method.” *Journal of Applied Mechanics,* **17**, (1950), 448–453.
9. R. D. Blevins. *Formulas for Natural Frequency and Mode Shape*. Krieger Publishing, 2001.
10. A. W. Leissa. *Vibration of Plates*. Tech. rep. NASA SP.160, Washington, 1969.
11. A. W. Leissa. “The free vibration of rectangular plates.” *Journal of Sound Vibration,* **31**, (1973), pp. 257–293. DOI: 10.1016/S0022-460X(73)80371-2.
12. A. O. Oyelade, O. M. Sadiq, and Fakinlede O. A. “Sound transmission through triple plates separated by air cavities in the low-frequency range.” *Acta Mechanica,* **230**, (2019), pp. 965–977. DOI: 10.1007/s00707-018-2318-9.
13. A. O. Oyelade, R. Yi C. Zhang, and G. Hu. “Analytical and experimental investigation on sound transmission of double thin plates with magnetic negative stiffness.” *International Journal of Applied Mechanics,* **10**, (2018), 1850054–1. DOI: 10.1142/S1758825118500540.